Stretching and heating single DNA molecules with optically trapped gold-silica Janus particles

Sabrina Simoncelli[1†‡], Samuel Johnson[1‡], Franziska Kriegel[2], Jan Lipfert[2,3*] and Jochen Feldmann[1,3]*

[1]Photonics and Optoelectronics Group, Department of Physics and Center for Nanoscience (CeNS), Ludwig-Maximilians-Universität München, Amalienstraße 54, Munich, 80799, Germany
[2]Department of Physics and Center for Nanoscience (CeNS), Ludwig-Maximilians-Universität München, Geschwister-Scholl-Platz 1, Munich, 80539, Germany
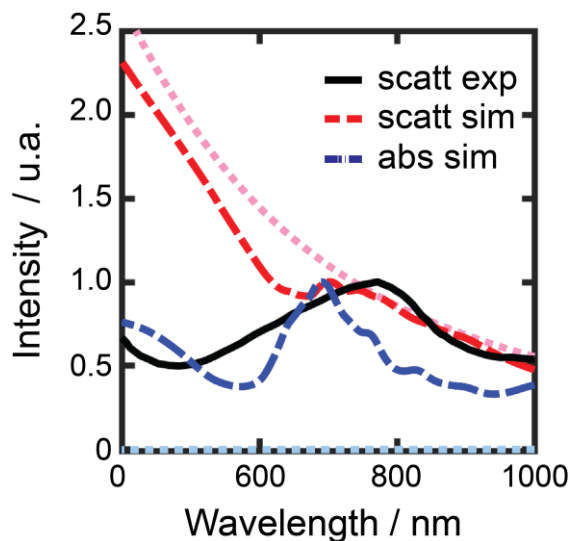[3]Nanosystems Initiative Munich (NIM), Schellingstraße 4, 80539 Munich, Germany
[‡]These authors contributed equally to this work
[†]Present address: The Blackett Laboratory, Department of Physics, Imperial College, London SW7 2AZ, UK.

Contents

S1: Optical characterization of Au-silica Janus particles

Figure S1. Simulated scattering (red dashed line) and absorption (blue dashed line) spectra of an individual 1.3 μm in diameter Au-silica Janus particle with a 5 nm thick gold half-coating in water. Representative white light scattering spectrum of an individual Au-silica Janus particle in water measured experimentally (black solid line). Simulated scattering (pink dotted line) and absorption (light-blue dotted line) spectra of an individual 1.3 μm in diameter bare silica sphere in water.

S2: Tethering efficiency of single DNA molecules to Au-silica Janus particles

To optimize the DNA:Janus stoichiometry to ~ 1:1 and to estimate the yield of the conjugation, we tested different reaction conditions (concentration of dsDNA and Janus particles; reaction time; temperature; buffer type and concentration) using a shorter DNA sequence (18 bp-long) and 50 nm gold nanoparticles (AuNPs) attached to one of the ssDNA molecules as a marker element. We used the high affinity biotin-streptavidin interaction to bind individual AuNP to a single ssDNA sequence. Streptavidin coated 50 nm gold nanoparticles were purchased from Nanopartz Inc. and 18 bp long biotin-labeled (multiple A sequence) and thiol-labeled (multiple T sequence) ssDNA were obtained from biomers.net. All the reactions were performed in a one-pot reaction by incubating overnight streptavidin coated AuNPs, Au-silica Janus particles, biotin-labeled multi A ssDNA and thiol-labeled multi T ssDNA in a PBS buffer solution at 4 ºC. To estimate the yield of the reaction, a drop of the reaction solution was casted over a scanning electron microscopy (SEM) silicon wafer and imaged in a Gemini Ultra Plus equipment (Zeiss). Prior to SEM imaging, a 2 nm gold−palladium layer was sputtered on the sample (20 s, 30 mA, 5 cm working distance).

Imaging was performed in SE2 and InLens modes at an electron acceleration voltage of 2 kV with a working distance of ~3 mm. Figure S2a depicts a representative wide-field SEM image of the reaction conditions that yielded an almost perfect Poisson distribution for the number of AuNP bound per Au-silica Janus particle. The concentration of Au-silica Janus particles, streptavidin coated AuNPs, thiol-ssDNA, biotin-ssDNA, sodium phosphate buffer and NaCl in the final solution was 12 fM, 0.6 pM, 100 pM, 100 pM, 5 mM and 7.5 mM, respectively. We imaged ~ 330 Janus particles and plotted in Figure S2b the distribution of the number of AuNPs tethered per Janus particle. We found that ~ 30 % of the Janus particles have exactly one AuNP (i.e. DNA molecule) tethered and that the number of Janus particles with more than one AuNP is negligible.
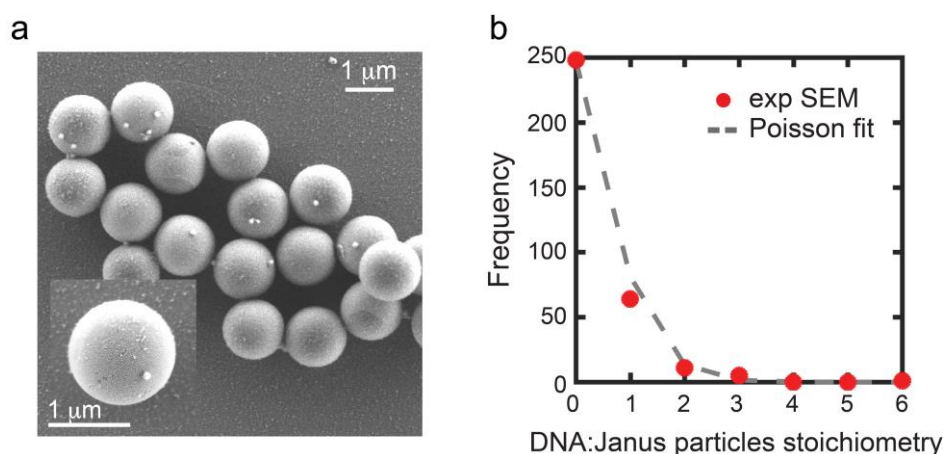

Figure S2. (a) Representative SEM image of 50 nm AuNPs tethered through DNA hybridization to Au-silica Janus particles. The inset shows an enlarged view of an individual 1:1 AuNP: Janus particle. (b) Efficiency of the DNA tethering following overnight incubation with Au-silica Janus particles as a function of the tether:particle stoichiometry. The DNA:Janus particle stoichiometry was determined by inspection of the number of AuNPs that bound to a single Au-silica Janus particle in the SEM images. The dashed line represents the Poisson fit to the experimental data (red circles).

S3: Forces acting on a free optically trapped Au-silica Janus particle

The height of a free gold-silica Janus particle in the optical trap is only determined by the equilibrium position given by the optical and the thermophoretic forces. The optical forces encompass the gradient force, which pushes the particle towards the position of maximum laser intensity, and the scattering force, which, is stronger in the gold-coated hemisphere of the particle, pushing it towards the direction of the beam propagation. The thermophoretic force arises from the self-generated thermal gradient between the gold and silica hemispheres. This self-thermal gradient moves the Janus particle upwards in the optical trap

as it acts against the thermal gradient. The sedimentation force, which is a combination of the gravitational and buoyancy forces, is practically negligible. Furthermore, we do not take into account the effect of the spherical aberrations at the water/glass slide interface because even for the lowest stable trapping laser power the Janus particle is always 1 µm above the surface of the cover-slide and therefore, this effect is negligible.

S4: Axial displacement of optically trapped DNA-tethered Au-silica Janus particles.
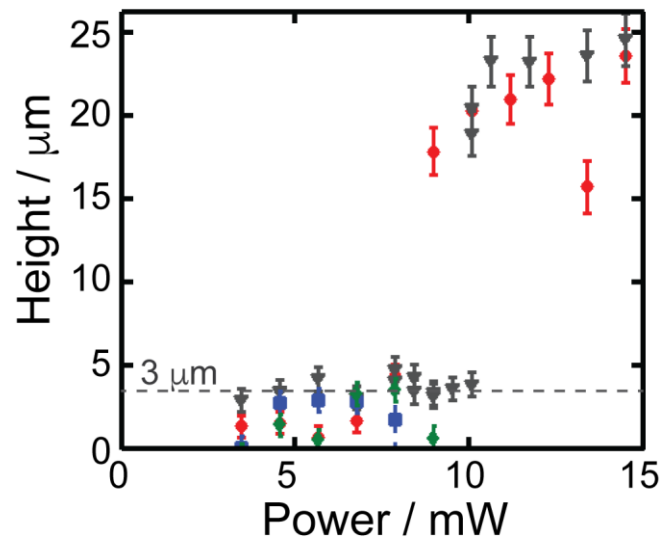
Figure S3. Axial displacement (height) of Au-silica Janus particles (diameter = 1.3 ± 0.1 µm) tethered to a glass substrate with a 3 µm in length dsDNA molecule. The different symbols represent the axial displacement behavior for individual DNA-tethered Janus particles. The blue and green data set corresponds to cases where the DNA-tether ruptured before being fully stretched and then the particle fell out of the optical trap.

S5: Axial optical forces in the limit of small radial displacements

For particles of size R much smaller than the wavelength of the trapping beam, λ, the gradient and scattering forces can be approximated using the dipole approximation (Rayleigh theory).[1] However, for the intermediate size regime studied in this work, $R \sim \lambda$, the dipole approximation predicts forces which could be typically off by a factor of 3-4 compared to experimental results.[2] For that reason, we decided to use the model derived by Tlusty *et al.*, which provides an accurate description of the gradient forces for these intermediate size regime.[3] In the limit of small radial displacements from the focus of the beam, r < 200 nm, the trapped particle can be simplified to a harmonic oscillator with a Hookean linear response. For a Gaussian beam of eccentricity ϵ the resulting axial and radial gradient force

constants, $k_{g,z}$ and $k_{g,r}$, are described by Equation 1 and 2, respectively,

$$k_{g,z} = \alpha I_0 \omega_0 \frac{2\pi}{\xi^3} \cdot \left[2a\xi^2 e^{\frac{-a^2}{2\epsilon^2}} - \sqrt{2\pi}\epsilon e^{\frac{-a^2}{2}} \text{erf}(\frac{a\xi}{\sqrt{2}\epsilon}) \right] \tag{1}$$

$$k_{g,r} = \alpha I_0 \omega_0 e^{\frac{-a^2}{2}} \frac{\pi\epsilon}{\xi^3} \cdot \left[-2a\epsilon\xi e^{\frac{-a^2\xi^2}{2\epsilon^2}} + \sqrt{2\pi}(\epsilon^2 + a^2\xi^2)\text{erf}(\frac{a\xi}{\sqrt{2}\epsilon}) \right] \tag{2}$$

where α is equal to $\varepsilon_p/\varepsilon_m - 1$ and accounts for the relative difference of the dielectric constants of the particle, ε_p, and the surrounding medium, ε_m; I_0 is the energy density of the applied electric field; ϵ is the eccentricity and is given by the ratio of the axial, ω, to the transverse, ω_0, beam waist in the focus (r = 0); a is R/ω_0, which is the normalized radius; and ξ is the anisotropy and equal to $\sqrt{1 - \epsilon^2}$.

In the radial direction, only gradient forces contribute to the optical potential of the trapped particle, such that,

$$F_r = k_{g,r}r \tag{3}$$

where *r* is the radial coordinate in typical cylindrical polar-coordinates.

On the other hand, the optical forces acting along the *z*-axis on an optically trapped Janus particle are the gradient force, $F_{g,z}$ and the scattering force, $F_{s,z}$. However, axial stable optical trapping requires the axial gradient forces to exceed the axial scattering forces. Assuming $F_{g,z}$ >> $F_{s,z}$ the total axial optical forces can be well approximated to the gradient forces as,

$$F_z = k_{g,z}z \tag{4}$$

where *z* is the height relative to the focus of the beam.

We note that the ratio of the axial and lateral trap stiffness, $k_{g,z}/k_{g,r}$, only depends on the size of the particle and the optical geometry of the system. The value of ω_0 was determined experimentally to be 780 ± 7 nm by fitting a Gaussian function to the detected signal of the trapping beam. Therefore, applying Equations 1 and 2 and using the experimentally determined values of the beam waist (ω_0 = 780 ± 7 nm) and the radius of the Janus particle (R = 650 nm) gives a value of 0.09 ± 0.01 for the $k_{g,z}/k_{g,r}$ ratio. The eccentricity ϵ was estimated using the paraxial Gaussian model as ϵ = 5.8. For our specific experimental conditions (ω_0 = 780 ± 7 nm and λ = 1064 nm) the paraxial approximation is accurate within < 10 %. [4]

S6: Thermophoretic force on free Au-silica Janus particles.
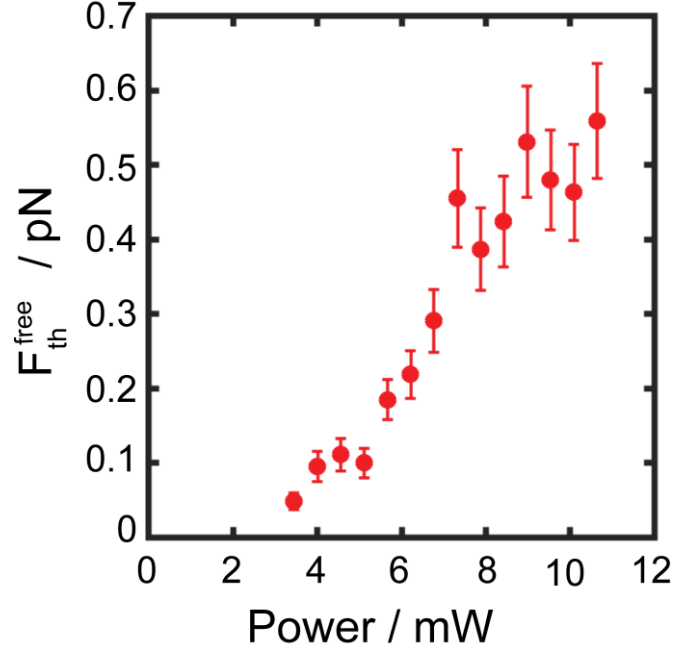
Figure S4. Thermophoretic force acting on free Au-silica Janus particles as a function of the trapping laser power.

S7: Thermophoretic force

To convert the thermophoretic force between the free and the DNA-tethered Janus particle we must consider the height differences between the two systems at a given laser power. The thermophoretic force, or Stokes drag force, is proportional to the temperature gradient, ∇T, and the Soret coefficient, S_T,

$$F_{th} = 6\pi R \eta v_{th} = k_B T S_T \nabla T \tag{5}$$

where R is the radio of the particle, η is the viscosity of the media and v_{th} is the thermophoretic mobility. The thermal gradient between the silica and gold hemisphere of the Janus particle is proportional to the laser intensity. The metallic hemisphere of Janus particles absorbs light and dissipates it as heat in the immediate surroundings. The difference of temperature between the two hemispheres of the particle is given by[5]

$$\Delta T = \frac{3\epsilon I R}{2(2\kappa_0 + \kappa_i)} \tag{6}$$

with ϵ being the absorption efficiency of the metallic layer, I the intensity of the trapping beam and κ_0 and κ_i the thermal conductivity inside and outside the particle, respectively. Finally the thermophoretic force can be described with the following equation following the derivation presented in the reference S5,[5]

$$F_{th} = \frac{k_B T S_T \Delta T}{3R} \tag{7}$$

S6

S8: Free to DNA-tethered thermophoretic force conversion

We considered our focused beam as a paraxial Gaussian beam propagating along the z direction. Therefore, the variation of the laser intensity as a function of the propagation length z is given by Equation 8.

$$I(0,z) = \frac{I_0}{1+(\frac{z}{z_0})^2} \tag{8}$$

where $z_0 = \pi w_0^2/\lambda_m$, $k_m = 2\pi/\lambda_m$ and λ_m is the wavelength of the light in the propagating medium. Combining Equation 6 and 7 results in,

$$F_{th} = \frac{k_B T S_T \epsilon I}{2(2\kappa_0 + \kappa_i)} \tag{9}$$

which finally leads to

$$F_{th}^{DNA}/F_{th}^{free} = I(h_{DNA})/I(h_{free}) \tag{10}$$

so that,

$$F_{th}^{DNA} = F_{th}^{free} \cdot \frac{z_0^2 + \Delta h_{free}^2}{z_0^2 + \Delta h_{DNA}^2} \tag{11}$$

In order to use this equation for all the trapping laser powers of the experiment, we extrapolated the height of the free Janus particles for powers after the jump, to the linear fit of the height versus power for the free Janus particles before the jump. This allows us to use Equation 8 for all the powers to describe the dependence of the laser intensity with the axial position.

## S9: Force-extension curve of a partially de-hybridized DNA molecule

The total extension, l, of a partially de-hybridized DNA molecule is given by the sum of the extensions of the dsDNA, l_{ds}, and ssDNA, l_{ss}, sections at a given tension F,

$$l(F) = l_{ds}(F) \cdot x_{ds} + l_{ss}(F) \cdot x_{ss} \tag{12}$$

where x_{ds} and x_{ss} corresponds to the fraction of double- and single-stranded DNA, respectively. The extension of the ds- and ssDNA sections are given by the worm-like chain (WLC) model.[6] We use the typical value of 1000 pN,[7] and 900 pN[8] for the stretch modulus of ds- and ssDNA, respectively.

S10: Temperature distribution around an optically trapped Janus particle

Fluorescent proteins are often used for measuring intracellular temperatures due to the thermal sensitivity of its fluorescent. Specifically, the fluorescence of the red fluorescence protein decreases linearly with an increase in temperature at a rate given by -1.28 %/°C.[9] The protein emits light at 588 nm and it can be excited with a 532 nm laser. Therefore, to measure the fluorescence intensity of the protein in the vicinity of an optically trap Janus particle, we superimposed an expanded 532 nm laser beam (beam waist ~ 13 μm) with the 1064 nm trapping laser. First, we locate and optically trap the Janus particle. Then, we turn off the white light source used in the dark-field microscopy configuration and switch on the 532 nm laser to monitor the fluorescence of the red fluorescent protein. The Janus particle is optically trapped during the whole time interval of the measurement. The orientation of the Janus particle in the optical trap is always with the gold hemisphere facing towards the light propagation direction. However, slightly rotations of the Janus particle in the optical trap allow us to image the fluorescence intensity around the gold and silica hemisphere simultaneously. In the following section we only analyzed these situations. Figure S3a displays the spatial fluorescence distribution of the red fluorescent protein in the near vicinity of an optically trapped Au-silica Janus particle (with a trapping laser power of 3.5 mW). As depicted in Figure S5, the fluorescence of the red fluorescent protein is not homogenous around the optically trapped Janus particle. Each image corresponds to a different rotational orientation of the Janus particle inside the optical trap. To quantify the decrease in the fluorescence signal around the gold-coated hemisphere we discarded the fluorescence signal over the trapped Janus particle, and we fitted with a Gaussian function of identical width to the fluorescence profiles around the gold and silica side, respectively (Fig. S3b). The fluorescence signal around the gold hemisphere is ~ 15 ± 3 % lower than the fluorescence signal around the silica hemisphere, for a trapping laser power of 3.5 mW. This fluorescence decrease corresponds to a temperature increase of 8 ± 4 K. Further plasmonic heating under 532 nm laser excitation can be excluded because, even though the absorption cross section of Au-silica Janus particles at 532 nm and 1064 nm is fairly similar (Figure S1), the power density of the 532 nm laser is 200 times lower than the power density of the 1064 nm optical trapping laser.
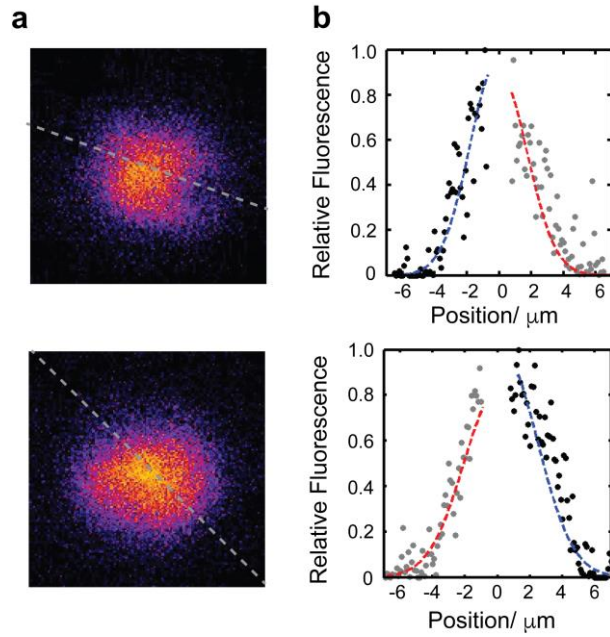
Figure S5. (a) Fluorescence distribution of red fluorescent protein around an optically trapped Au-silica Janus particle. The red fluorescence protein acts as an in-situ temperature sensor and it is excited using an expanded 532 nm laser that is superimposed to the 1064 nm trapping beam. The upper and bottom images correspond to two different rotational orientations of the Janus particle inside the optical trap. The dimensions of the images are 15.7 x 15.7 μm^2. The power outputs (and power densities) of the green and IR laser beams are 0.4 (1 $\mu W/\mu m^2$) and 3.5 mW (200 $\mu W/\mu m^2$), respectively. (b) Normalized fluorescence intensity profiles of red fluorescence protein across the grey dashed lines presented in a. The fluorescence signal over the Janus particles was discarded. The dashed lines correspond to the Gaussian fits of the experimental data around the silica (blue) and gold-coated (red) hemispheres of the Janus particle.

S11: Melting curve of the 9-kb-long dsDNA
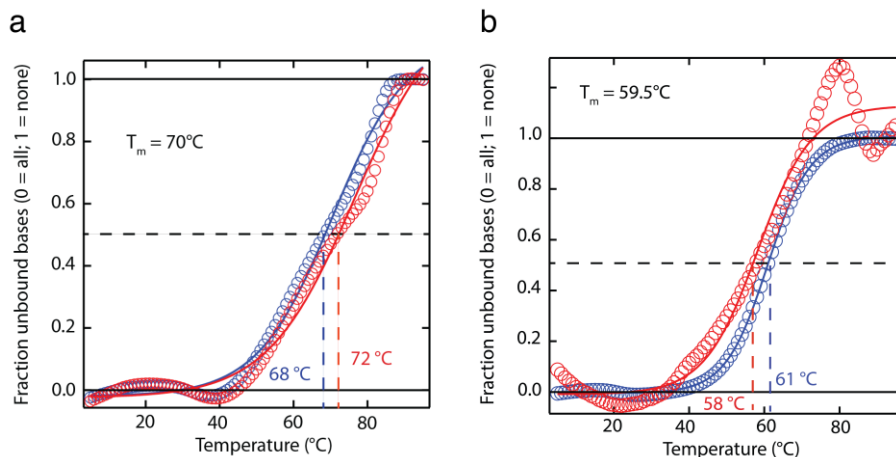
Figure S6. Melting curve for the 9-kb-long dsDNA construct used for Janus particle-based stretching experiments. The data corresponds to the fraction of "unpaired bases" as a function of the temperature. Blue and red illustrate the data recorded going down from 95 to 5 °C and up from 5 to 95 °C, respectively. The presence of some hysteresis in the data is explained by

the still relative short measurement time at each temperature step (one minute per degree Celsius). The melting temperature is defined as the temperature at which 50 % of the bases are molten (indicated by the black dashed line). The melting temperature T_m was calculated by taking the mean of the fitted melting temperatures from the cooling and the heating traces and it is 70 ± 2 °C at 150 mM Na$^+$ concentration (a) and 59.5 ± 1.5 °C at 7.5 mM Na$^+$ concentration (b). The salt concentration used in the single-molecule experiments is 7.5 mM Na$^+$.

S12: Lifetime of DIG-antiDIG bond.
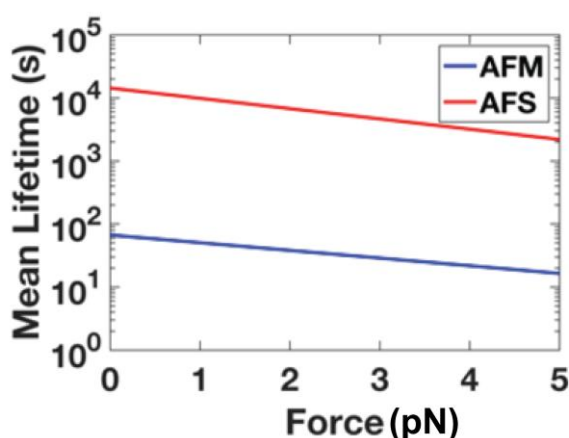
Figure S7. Mean lifetime of DIG-antiDIG bond as a function of the applied force. The plot was generated using the results of Wuite and coworkers[10] and Gaub and coworkers[11] who measured the DIG-antiDIG bond lifetime using acoustic force spectroscopy (AFS) and atomic force microscopy (AFM), respectively.

Supplementary References

(S1)   Agayan, R. R.; Gittes, F.; Kopelman, R.; Schmidt, C. F. Optical Trapping near Resonance Absorption. *Appl. Opt.* **2002**, *41*, 2318.
(S2)   Svoboda, K.; Block, S. M. Biological Applications of Optical Forces. *Annu. Rev. Biophys. Biomol. Struct.* **1994**, *23*, 247–285.
(S3)   Tlusty, T.; Meller, A.; Bar-Ziv, R. Optical Gradient Forces of Strongly Localized Fields. *Phys. Rev. Lett.* **1998**, *81*, 1738–1741.
(S4)   Barton, J. P.; Alexander, D. R. Fifth-Order Corrected Electromagnetic Field Components for a Fundamental Gaussian Beam. *J. Appl. Phys.* **1989**, *66*, 2800–2802.
(S5)   Jiang, H. R.; Yoshinaga, N.; Sano, M. Active Motion of a Janus Particle by Self-Thermophoresis in a Defocused Laser Beam. *Phys. Rev. Lett.* **2010**, *105*, 268302.
(S6)   Petrosyan, R. Improved Approximations for Some Polymer Extension Models. *Rheologica Acta*, **2016**, 1–6.
(S7)   Wang, M. D.; Yin, H.; Landick, R.; Gelles, J.; Block, S. M. Stretching DNA with Optical Tweezers. *Biophys. J.* **1997**, *72*, 1335–1346.
(S8)   Zhang, Y.; Zhou, H.; Ou-Yang, Z. C. Stretching Single-Stranded DNA: Interplay of Electrostatic, Base-Pairing, and Base-Pair Stacking Interactions. *Biophys. J.* **2001**, *81*, 1133–1143.
(S9)   Deepankumar, K.; Nadarajan, S. P.; Bae, D.-H.; Baek, K.-H.; Choi, K.-Y.; Yun, H.

Temperature Sensing Using Red Fluorescent Protein. *Biotechnol. Bioprocess Eng.* **2015**, *20*, 67–72.

(S10) Sitters, G.; Kamsma, D.; Thalhammer, G.; Ritsch-Marte, M.; Peterman, E. J. G.; Wuite, G. J. L. Acoustic Force Spectroscopy. *Nat. Methods* **2015**, *12*, 47–50.

(S11) Neuert, G.; Albrecht, C.; Pamir, E.; Gaub, H. E. Dynamic Force Spectroscopy of the Digoxigenin-Antibody Complex. *FEBS Lett.* **2006**, *580*, 505–509.